Available at
www.ComputerScienceWeb.com
POWERED BY SCIENCE DIRECT

ELSEVIER

Signal Processing 83 (2003) 1643 – 1659

SIGNAL PROCESSING

www.elsevier.com/locate/sigpro

Impulse shortening and equalization of frequency-selective MIMO channels with respect to layered space–time architectures☆

Dirk Wübben[a,*], Karl-Dirk Kammeyer[a]

[a] *Department of Communications Engineering, University of Bremen, P.O.Box 33 04 40, 28334 Bremen, Germany*

Received 15 September 2002; received in revised form 17 December 2002

Dedicated to Prof. em. Dr.-Ing., Dr.-Ing.e.h., Dr. techn.e.h. Hans Wilhelm Schüßler on occasion of his 75th birthday

Abstract

Multiple antenna systems may be used in fading environments to exploit an enormous capacity advantage. Most of the coding schemes and transmission architectures published so far have been restricted to non-frequency-selective fading channels. For adopting these narrowband schemes to frequency-selective environments, appropriate algorithms to mitigate the influence of inter-layer interference and intersymbol interference have to be investigated. In this paper, we give a survey of existing algorithms to shorten the effective channel impulse response and to equalize frequency-selective MIMO channels. In addition, a successive detection algorithm similar to V-BLAST is viewed and a new improved iterative algorithm is proposed. This algorithm is called Frequency-Selective Backward Iterative cancellation and achieves an enlarged detection diversity. The main object of this investigation is to represent the different systematics and to compare these schemes with respect to simulated bit error rates.

1. Introduction

In a Rayleigh fading environment multiple antenna systems provide an enormous increase in capacity compared to single antenna systems [20]. Consequently, multiple-input multiple-output (MIMO) systems are predestined for high data rate wireless communications. To exploit this potential, Foschini proposed a MIMO system containing a diagonally layered coding structure named D-BLAST (*Diagonal Bell Labs Layered Space Time*) [12]. A simplified scheme was proposed in [22] and is known as V-BLAST (*Vertical* BLAST), which associates each layer with a specific transmit antenna.

Recently, a discussion started to consider these algorithms also in the broadband regime where the signal bandwidth exceeds the coherence bandwidth of the channel. Therefore, appropriate algorithms to mitigate the influence of ILI (inter-layer interference) and ISI (intersymbol interference) for each transmit signal have to be investigated. From the literature different approaches are known: MLSE in space–time-domain, orthogonal frequency division multiplexing (OFDM),

☆ This work was supported by the German ministry of education and research (BMBF) within the project HyEff (project No. 01 BU 153).

* Corresponding author. Tel.: +49-421-218-2545; fax: +49-421-218-3341.

E-mail addresses: wuebben@ant.uni-bremen.de (D. Wübben), kammeyer@ant.uni-bremen.de (K.-D. Kammeyer).

0165-1684/03/$ - see front matter © 2003 Elsevier Science B.V. All rights reserved.
doi:10.1016/S0165-1684(03)00084-7

equalization in frequency-domain, and equalization in time-domain. The first approach has been proposed in [21] utilizing a vector version of the Viterbi algorithm but suffers from an enormous complexity. The second approach transforms the frequency-selective MIMO channel into a large number of parallel and approximately flat-fading MIMO channels using the inverse fast Fourier transform (IFFT) at the transmitter and the FFT at the receiver [15,18]. A comparative study of equalization schemes in the frequency-domain utilizing the FFT and IFFT, but both at the receiver, is given in [9]. In this paper we concentrate on the fourth approach, i.e., equalization in time-domain using a FIR filter at the receiver for impulse shortening.

Impulse shortening algorithms using a FIR pre-filter at the receiver have been well studied for single-input single-output (SISO) transmission [2,11,14]. They provide an elegant solution to shorten the (effective) channel memory utilizing a time-domain equalizer and results in a reduced number of states for a Viterbi equalizer. [1] Due to the decreased number of states, the computational complexity of the equalizer significantly diminishes. Furthermore, time-domain pre-filter can be used in OFDM transmission schemes to reduce the required cyclic prefix length and therefore increases the data rate due to the reduced overhead [19].

The extension of impulse shortening filters to MIMO channels has been presented in [1,3–6,17]. The proposed algorithms reduce the effective channel memory and may be used as prefilter for MIMO-OFDM schemes. In addition, some of these algorithms provide a MIMO-DFE structure and, consequently, allow the immediate equalization of ILI and ISI in space–time-domain.

Apart from these channel shortening algorithms, an additional approach of using space-time filtering at the receiver has been proposed to detect frequency-selective MIMO systems [16,17]. This scheme represents a generalization of the V-BLAST detection algorithm for frequency-selective fading channels. It is based on a multiple-input single-output (MISO) decision feedback structure to detect the distinct layers in a successive way. We call it frequency-selective BLAST (FS-BLAST) throughout this paper. An iterative extension of this algorithm is proposed in the subsequent called Frequency-Selective Backward Iterative Cancellation (FS-BIC). This FS-BIC significantly improves the performance of FS-BLAST by increasing the detection diversity step-by-step.

The remainder of this paper is organized as follows. The MIMO system is described in Section 2 and the impulse shortening algorithms are viewed in Section 3. The filter definitions are derived and the system performance is evaluated by simulation results. The FS-BLAST architecture and the new approach FS-BIC are introduced in Section 4. The performance of FS-BLAST is compared with the impulse shortening algorithms and the improvement of the iterative scheme is investigated. A summary and conclusion marks can be found in Section 5.

2. System description

2.1. Layered space–time architecture

We consider the frequency-selective (FS) multiple antenna system with n_{T} transmit and $n_{\mathrm{R}} \geqslant n_{\mathrm{T}}$ receive antennas shown in Fig. 1. The data is demultiplexed in n_{T} data substreams of equal length (called layers) and these uncoded substreams are mapped into M-PSK or M-QAM symbols. The data symbols are organized in frames of equal length and are transmitted over the n_{T} antennas at the same time. The transmitter equals the V-BLAST system [22–24] and is denoted as layered space–time architecture.

To derive the input–output relation for this frequency-selective transmission system, two different models are introduced in the subsequent paragraphs.

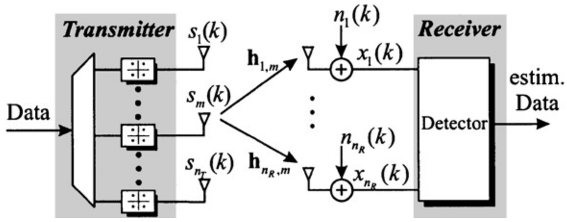

Fig. 1. Model of a frequency-selective MIMO system with n_{T} transmit and n_{R} receive antennas.

[1] Due to impulse shortening the Viterbi provides only *near-maximum-likelihood* performance, thus the Viterbi is named *near* MLSE (maximum-likelihood sequence estimator) detector.

The first model describes the FS system as a linear superposition of several flat-fading MIMO systems, whereas the second model uses a linear combination of n_T frequency-selective single-input multiple-output (SIMO) systems.

2.2. MIMO input–output model

In order to describe the FS-MIMO system, we denote the symbol transmitted by antenna m at time instant k by $s_m(k)$ with average symbol energy σ_s^2 and likewise the signal received at antenna n is indicated by $x_n(k)$. The frequency-selective single-input single-output (SISO) channel impulse response (CIR) from transmit antenna m to receive antenna n is given by the $(L+1) \times 1$ vector[2] $\mathbf{h}_{n,m} = [h_{n,m}(0)\ h_{n,m}(1)\ \ldots\ h_{n,m}(L)]^{\mathrm{T}}$. For simplicity, we assume the same channel order L for all SISO channels $\mathbf{h}_{n,m}$. It is further assumed that the channel is constant over the frame length, but may change from frame to frame (*block fading channel*) and is perfectly known by the receiver. The power normalization ($E\{\|\mathbf{h}_{n,m}\|^2\}=1$) is used for the i.i.d. complex channel coefficients of each SISO channel. For this each SISO channel is modelled by L statistically independent Rayleigh fading processes with equal average power (Fig. 1).

The n_T transmitted symbols at time instant k are collected in the $n_T \times 1$ vector

$$\mathbf{s}(k) = \begin{bmatrix} s_1(k) \\ \vdots \\ s_{n_T}(k) \end{bmatrix} \tag{1}$$

and correspondingly the $n_R \times 1$ received signal vector

$$\mathbf{x}(k) = \begin{bmatrix} x_1(k) \\ \vdots \\ x_{n_R}(k) \end{bmatrix} \tag{2}$$

describes the n_R received signals at the same time. This receive vector contains a linear superposition of the delayed transmit vectors $\mathbf{s}(k-l)$ with tap delay $0 \leqslant l \leqslant L$ and is calculated by

$$\mathbf{x}(k) = \sum_{l=0}^{L} \mathbf{H}(l)\mathbf{s}(k-l) + \mathbf{n}(k). \tag{3}$$

In (3), $\mathbf{n}(k)$ labels the noise vector at the n_R receive antennas at symbol time k, assuming uncorrelated white Gaussian noise and spatial covariance $E\{\mathbf{n}(k)\mathbf{n}^{\mathrm{H}}(k)\} = \sigma_n^2 \mathbf{I}_{n_R}$. The $n_R \times n_T$ MIMO matrix

$$\mathbf{H}(l) = \begin{bmatrix} h_{1,1}(l) & \cdots & h_{1,n_T}(l) \\ \vdots & \ddots & \vdots \\ h_{n_R,1}(l) & \cdots & h_{n_R,n_T}(l) \end{bmatrix} \tag{4}$$

is a function of the index l, where $0 \leqslant l \leqslant L$. Thus, the FS system is viewed as a superposition of $L+1$ non-frequency-selective MIMO systems and noise. As an alternative, a second input–output model as a superposition of n_T SIMO transmissions is introduced in the next paragraph.

2.3. SIMO input–output model

To describe the input–output relation between transmit antenna m and all n_R receive antennas the $n_R \times (L+1)$ SIMO channel matrix

$$\mathbf{H}_m = \begin{bmatrix} \mathbf{h}_{1,m}^{\mathrm{T}} \\ \vdots \\ \mathbf{h}_{n_R,m}^{\mathrm{T}} \end{bmatrix} \tag{5}$$

is defined. With the *sequence* of $L+1$ symbols transmitted by antenna m

$$\mathbf{s}_m(k) = \begin{bmatrix} s_m(k) \\ \vdots \\ s_m(k-L) \end{bmatrix} \tag{6}$$

the $n_R \times 1$ received signal vector $\mathbf{x}(k)$ in (2) becomes a linear superposition of n_T SIMO transmissions and noise:

$$\mathbf{x}(k) = \sum_{m=1}^{n_T} \mathbf{H}_m \mathbf{s}_m(k) + \mathbf{n}(k). \tag{7}$$

Of course, (7) corresponds to (3) as both equations describe the same transmission scheme. The main

[2] Throughout the remainder, $(\cdot)^*$, $(\cdot)^{\mathrm{T}}$ and $(\cdot)^{\mathrm{H}}$ denote the conjugation, the matrix transposition and the hermitian transposition, respectively. Furthermore $\mathbf{I}_\alpha$ indicates the $\alpha \times \alpha$ identity matrix and $\mathbf{0}_{\alpha,\beta}$ denotes the $\alpha \times \beta$ all zero matrix.

difference lies in the alignment of the transmit signals and the channel coefficients, respectively. As we shall see in the derivation of the different prefilters, these two signal arrangements lead to compact filter definitions.

3. MIMO impulse shortening

3.1. Principle of impulse shortening

Reducing the effective length of a channel impulse response by applying FIR filtering at the receiver has been adopted for SISO channels in a number of publications, e.g. [2,11,14]. The basic idea is to apply a linear prefilter (called impulse shortening filter, ISF) at the receiver, so that the serial concatenation of the transmission channel and the ISF has an overall impulse response with less effective taps. Therefore the filter cascade can be described by a target impulse response (TIR) with a shorter impulse response length, which results in less computational effort for *near* MLSE detection.

The idea of impulse truncation has also been adopted for MIMO systems in several publications (e.g. [1,3–6,17]) using a two dimensional space–time filter to reduce the effective channel memory. Consequently, the aim of channel shortening is now to transform the $n_R \times n_T$ MIMO system of order L into a target system with n_T transmit and n_S equivalent receive antennas [3] of order $L_S \leqslant L$ [5,6].

A block diagram of equalizing the received signal $\mathbf{x}(k)$ with a space–time prefilter $\mathbf{W}$ is shown in Fig. 2, where $\mathbf{B}$ denotes the target impulse response and k_0 is an optional decision delay.

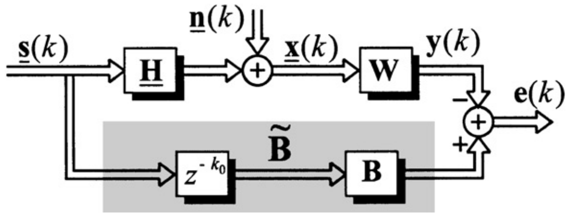

Fig. 2. Block diagram of the MIMO impulse shortening scheme defined by the impulse shortening filter $\mathbf{W}$ and the target impulse response $\mathbf{B}$.

3.2. Filter design

In order to calculate the ISF and the TIR, the MIMO input–output model defined in Section 2.2 is used. A impulse shortening scheme using the SIMO model proposed in Section 2.3 has been derived in [17].

3.2.1. Describing a sequence of received signals

To describe an input sequence of the MIMO impulse shortening filter $\mathbf{W}$, the input–output relation in (3) has to be extended to describe a *sequence* of received signals. With regard to the ISF order N, we denote the sequence of $N+1$ received signals by the $n_R(N+1) \times 1$ vector

$$\underline{\mathbf{x}}(k) = \begin{bmatrix} \mathbf{x}(k) \\ \vdots \\ \mathbf{x}(k-N) \end{bmatrix} \tag{8}$$

and the sequence of $N+L+1$ transmit vectors (1) by the $n_T(N+L+1) \times 1$ vector

$$\underline{\mathbf{s}}(k) = \begin{bmatrix} \mathbf{s}(k) \\ \vdots \\ \mathbf{s}(k-N-L) \end{bmatrix}. \tag{9}$$

By defining the $n_R(N+1) \times n_T(N+L+1)$ block Toeplitz matrix

$$\underline{\mathbf{H}} = \begin{bmatrix} \mathbf{H}(0) & \cdots & \mathbf{H}(L) & \mathbf{0} & \mathbf{0} \\ \mathbf{0} & \mathbf{H}(0) & \cdots & \mathbf{H}(L) & \vdots \\ \vdots & & & & \vdots \\ \mathbf{0} & \cdots & \mathbf{H}(0) & \cdots & \mathbf{H}(L) \end{bmatrix} \tag{10}$$

and the sequence of noise vectors $\underline{\mathbf{n}}(k)$ we can calculate the sequence of $N+1$ received vectors by

$$\underline{\mathbf{x}}(k) = \underline{\mathbf{H}}\ \underline{\mathbf{s}}(k) + \underline{\mathbf{n}}(k). \tag{11}$$

With respect to later derivations, we define the $n_T(N+L+1) \times n_T(N+L+1)$ input autocorrelation

[3] The number of filter output signals n_S will be specified later on in the derivation of the ISF and will be furthermore equated to the number of transmit antennas n_T for the detection schemes viewed in Section 3.3.

matrix $\mathbf{R}_{ss}=E\{\underline{\mathbf{s}}(k)\underline{\mathbf{s}}^{\mathrm{H}}(k)\}$ and the $n_{\mathrm{R}}(N+1)\times n_{\mathrm{R}}(N+1)$ noise correlation $\mathbf{R}_{nn}=E\{\underline{\mathbf{n}}(k)\underline{\mathbf{n}}^{\mathrm{H}}(k)\}$. Both are assumed to be nonsingular. Furthermore, we introduce the $n_{\mathrm{T}}(N+L+1)\times n_{\mathrm{R}}(N+1)$ input–output cross-correlation

$$\begin{aligned}\mathbf{R}_{sx} &= E\{\underline{\mathbf{s}}(k)\underline{\mathbf{x}}^{\mathrm{H}}(k)\}\\ &= E\{\underline{\mathbf{s}}(k)(\underline{\mathbf{H}}\ \underline{\mathbf{s}}(k)+\mathbf{n}(k))^{\mathrm{H}}\}\\ &= \mathbf{R}_{ss}\mathbf{H}^{\mathrm{H}}\end{aligned} \tag{12}$$

and the $n_{\mathrm{R}}(N+1)\times n_{\mathrm{R}}(N+1)$ output autocorrelation

$$\begin{aligned}\mathbf{R}_{xx} &= E\{\underline{\mathbf{x}}(k)\underline{\mathbf{x}}^{\mathrm{H}}(k)\}\\ &= E\{(\underline{\mathbf{H}}\ \underline{\mathbf{s}}(k)+\mathbf{n}(k))(\underline{\mathbf{H}}\ \underline{\mathbf{s}}(k)+\mathbf{n}(k))^{\mathrm{H}}\}\\ &= \underline{\mathbf{H}}\mathbf{R}_{ss}\underline{\mathbf{H}}^{\mathrm{H}}+\mathbf{R}_{nn}.\end{aligned} \tag{13}$$

3.2.2. Derivation of impulse shortening filter W

As shown in Fig. 2, the sequence of received signals $\mathbf{x}(k)$ is filtered by a two-dimensional (space and time domain) impulse shortening filter $\mathbf{W}$ of order N. The n_{S} output signals of this ISF are calculated by

$$\mathbf{y}(k)=\sum_{l=0}^{N}\mathbf{W}(l)\mathbf{x}(k-l)=\mathbf{W}\underline{\mathbf{x}}(k). \tag{14}$$

with $\mathbf{y}(k)=[y_1(k),\dots,y_{n_{\mathrm{S}}}(k)]^{\mathrm{T}}$ denoting the $n_{\mathrm{S}}\times 1$ output vector. The ISF is defined by $N+1$ filter taps $\mathbf{W}(l)$

$$\mathbf{W}(l)=\begin{bmatrix} w_{1,1}(l) & \cdots & w_{1,n_{\mathrm{R}}}(l)\\ \vdots & \vdots & \vdots\\ w_{n_{\mathrm{S}},1}(l) & \cdots & w_{n_{\mathrm{S}},n_{\mathrm{R}}}(l)\end{bmatrix} \tag{15}$$

each of dimension $n_{\mathrm{S}}\times n_{\mathrm{R}}$ and the complete space-time filter of dimension $n_{\mathrm{S}}\times n_{\mathrm{R}}(N+1)$ is denoted by $\mathbf{W}=[\mathbf{W}(0)\ \ \mathbf{W}(1)\ \ \dots\ \ \mathbf{W}(N)]$. A detailed block diagram of MIMO filtering for an ISF with $n_{\mathrm{S}}=4$ output layers is shown in Fig. 3.

The cascade of the MIMO channel $\underline{\mathbf{H}}$ and the ISF $\mathbf{W}$ can be viewed as a MIMO channel with n_{T} transmit and n_{S} equivalent receive antennas. For the special case of $n_{\mathrm{S}}=n_{\mathrm{T}}$ the space–time prefilter has been derived in [1,4], whereas this restriction was relaxed in [5,6]. We will use this relaxed condition for the filter derivation and specify it later on due to the different receiver structures.

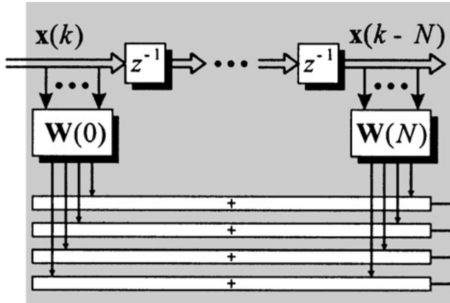

Fig. 3. Space–time filtering of the received signals $\mathbf{x}(k-l)$ with $N+1$ matrix taps $\mathbf{W}(l)$ to create $n_{\mathrm{S}}=4$ output signals $y_i(k)$.

Obviously, the aim of designing the ISF $\mathbf{W}$ is to equalize the given MIMO channel matrix $\underline{\mathbf{H}}$ to a target impulse response with $L_{\mathrm{S}}\leqslant L$ matrix taps. This target system is denoted by the $n_{\mathrm{S}}\times n_{\mathrm{T}}(L_{\mathrm{S}}+1)$ filter matrix $\mathbf{B}=[\mathbf{B}(0)\ \ \mathbf{B}(1)\ \ \dots\ \ \mathbf{B}(L_{\mathrm{S}})]$ containing the $n_{\mathrm{S}}\times n_{\mathrm{T}}$ space-only matrix taps $\mathbf{B}(l)$

$$\mathbf{B}(l)=\begin{bmatrix} b_{1,1}(l) & \cdots & b_{1,n_{\mathrm{T}}}(l)\\ \vdots & \vdots & \vdots\\ b_{n_{\mathrm{S}},1}(l) & \cdots & b_{n_{\mathrm{S}},n_{\mathrm{T}}}(l)\end{bmatrix}. \tag{16}$$

The input of this filter is given by the *sequence* of $L_{\mathrm{S}}+1$ transmit vectors delayed by k_0 time steps. For this we define the corresponding $n_{\mathrm{T}}(L_{\mathrm{S}}+1)\times 1$ input vector

$$\underline{\tilde{\mathbf{s}}}(k-k_0)=\begin{bmatrix}\mathbf{s}(k-k_0)\\ \vdots\\ \mathbf{s}(k-k_0-L_{\mathrm{S}})\end{bmatrix}=\mathbf{\Delta}_{k_0}\underline{\mathbf{s}}(k) \tag{17}$$

which can be factorized into the window matrix [4]

$$\mathbf{\Delta}_{k_0}=[\mathbf{0}_{n_{\mathrm{T}}(L_{\mathrm{S}}+1)\times n_{\mathrm{T}}k_0}\quad \mathbf{I}_{n_{\mathrm{T}}(L_{\mathrm{S}}+1)}\quad \mathbf{0}_{n_{\mathrm{T}}(L_{\mathrm{S}}+1)\times n_{\mathrm{T}}\delta}] \tag{18}$$

of dimension $n_{\mathrm{T}}(L_{\mathrm{S}}+1)\times n_{\mathrm{T}}(L+N+1)$ and the transmit sequence $\underline{\mathbf{s}}(k)$ introduced in (9). Consequently, the aim of the window matrix is the extraction of $L_{\mathrm{S}}+1$ consecutive transmit vectors from the sequence of $N+L+1$ transmit vectors, parameterized by the delay k_0. As already known for SISO impulse shortening, optimizing this delay k_0 has a deep impact on the performance of the receiver structure. Later on, the minimization of the mean square error (MSE) is used

[4] Parameter δ is determined by $\delta=N+L-L_{\mathrm{S}}-k_0$.

to optimize the delay in the range $0 \leqslant k_0 \leqslant N + L - L_S$ which results in a maximum signal-to-noise ratio (SNR) at the equalizer output [1,4].

Since the target system $\mathbf{B}$ considers only $L_S + 1 \leqslant L + 1$ taps for each SISO subchannel, an error between ISF output and TIR output occurs. To indicate this error we define the $n_S \times 1$ error vector (see Fig. 2)

$$\begin{aligned}\mathbf{e}(k) &= \mathbf{B}\tilde{\underline{\mathbf{s}}}(k-k_0) - \mathbf{W}\underline{\mathbf{x}}(k)\\ &= \mathbf{B}\boldsymbol{\Delta}_{k_0}\underline{\mathbf{s}}(k) - \mathbf{W}\underline{\mathbf{x}}(k) \qquad (19)\\ &= \tilde{\mathbf{B}}\underline{\mathbf{s}}(k) - \mathbf{W}\underline{\mathbf{x}}(k) \qquad (20)\end{aligned}$$

by applying (17) in the second line and utilizing the definition

$$\tilde{\mathbf{B}} = \mathbf{B}\boldsymbol{\Delta}_{k_0} = [\mathbf{0}_{n_S\times n_T k_0} \quad \mathbf{B} \quad \mathbf{0}_{n_S\times n_T\delta}] \qquad (21)$$

in the last line. Filter matrix $\tilde{\mathbf{B}}$ is of dimension $n_S \times (N + L + 1)$ and represents the idealized serial concatenation of $\underline{\mathbf{H}}$ and $\mathbf{W}$ with n_S output layers and contains only $L_S + 1$ effective matrix taps denoted by $\mathbf{B}$. In contrast, the real concatenation of $\underline{\mathbf{H}}$ and $\mathbf{W}$ generally leads to more than $L_S + 1$ matrix taps unequal to zero and thus affects the error vector $\mathbf{e}(k)$.

Using the definition of the error vector, the optimal filter $\mathbf{W}_{\rm opt}$ is calculated by using the orthogonality principle [13], which states that the optimal error vector is orthogonal to the observed data, i.e. $E\{\mathbf{e}(k)\mathbf{x}^{\rm H}(k)\} = \mathbf{0}$. Using (20) we obtain

$$\begin{aligned}E\{\mathbf{e}(k)\mathbf{x}^{\rm H}(k)\} &= E\{(\tilde{\mathbf{B}}\underline{\mathbf{s}}(k) - \mathbf{W}\underline{\mathbf{x}}(k))\underline{\mathbf{x}}^{\rm H}(k)\}\\ &= \tilde{\mathbf{B}}\mathbf{R}_{sx} - \mathbf{W}\mathbf{R}_{xx} = 0 \qquad (22)\end{aligned}$$

with the input–output cross-correlation $\mathbf{R}_{sx}$ and the output autocorrelation $\mathbf{R}_{xx}$, respectively. By solving (22) we achieve a well-defined relation between the two filter matrices:

$$\begin{aligned}\mathbf{W}_{\rm opt} &= \tilde{\mathbf{B}}\mathbf{R}_{sx}\mathbf{R}_{xx}^{-1}\\ &= \tilde{\mathbf{B}}\mathbf{R}_{ss}\mathbf{H}^{\rm H}(\mathbf{H}\mathbf{R}_{ss}\mathbf{H}^{\rm H} + \mathbf{R}_{nn})^{-1}\\ &= \tilde{\mathbf{B}}(\mathbf{R}_{ss}^{-1} + \mathbf{H}^{\rm H}\mathbf{R}_{nn}^{-1}\mathbf{H})^{-1}\mathbf{H}^{\rm H}\mathbf{R}_{nn}^{-1}, \qquad (23)\end{aligned}$$

where (12) and (13) were used in the second line. The third line is achieved by means of the matrix inversion lemma.[5] Consequently, for a given $\tilde{\mathbf{B}}$ the optimal prefilter $\mathbf{W}_{\rm opt}$ is uniquely specified by (23) and from there we can concentrate on optimizing $\tilde{\mathbf{B}}$ in the sequel.

3.2.3. *Derivation of target impulse response* B

In order to derive the TIR $\mathbf{B}$ in the sense of minimizing the mean-square-error (MSE), the $n_S \times n_S$ error autocorrelation matrix $\mathbf{R}_{ee} = E\{\mathbf{e}(k)\mathbf{e}^{\rm H}(k)\}$ is introduced to define the filter output SNR [1].

$$\mathrm{SNR}_{\rm ISF} = \frac{(1/n_T(N + L + 1))\,\mathrm{trace}(\mathbf{R}_{ss})}{\frac{1}{n_S}\,\mathrm{trace}(\mathbf{R}_{ee})}. \qquad (24)$$

The maximization of $\mathrm{SNR}_{\rm ISF}$ is an appropriate condition[6] to optimize the target impulse response $\mathbf{B}$. Assuming uncorrelated data $\mathbf{R}_{ss} = \sigma_s^2\mathbf{I}_{n_T(N+L+1)}$ the maximization of $\mathrm{SNR}_{\rm ISF}$ obviously leads to minimizing the trace of $\mathbf{R}_{ee}$, which results in the general optimization problem [1]

$$\mathbf{B}_{\rm opt} = \arg\min_{\mathbf{B}} \mathrm{trace}\,(\mathbf{R}_{ee}). \qquad (25)$$

To avoid the trivial solution $\mathbf{B} = \mathbf{0}$, this optimization problem has to be solved with respect to additional constraints. Some common constraints have been derived in [1,4] and the resulting algorithms will be recalled in Section 3.3. In advance, the structure of the error autocorrelation is further investigated to get a better insight into the optimization problem.

Using $\mathbf{W}_{\rm opt} = \tilde{\mathbf{B}}\mathbf{R}_{sx}\mathbf{R}_{xx}^{-1}$ from (23), we can describe the error autocorrelation matrix by [1]

$$\begin{aligned}\mathbf{R}_{ee} &= E\{\mathbf{e}(k)\mathbf{e}(k)^{\rm H}\}\\ &= \tilde{\mathbf{B}}(\mathbf{R}_{ss} - \mathbf{R}_{sx}\mathbf{R}_{xx}^{-1}\mathbf{R}_{sx}^{\rm H})\tilde{\mathbf{B}}^{\rm H} \qquad (26)\\ &= \tilde{\mathbf{B}}\mathbf{R}^{\perp}\tilde{\mathbf{B}}^{\rm H}, \qquad (27)\end{aligned}$$

where the definition $\mathbf{R}^{\perp} = \mathbf{R}_{ss} - \mathbf{R}_{sx}\mathbf{R}_{xx}^{-1}\mathbf{R}_{sx}^{\rm H}$ was introduced in the last line. Using again (12) and (13) and applying the matrix inversion lemma, we can write for this $n_T(N + L + 1) \times n_T(N + L + 1)$ matrix

$$\begin{aligned}\mathbf{R}^{\perp} &= \mathbf{R}_{ss} - \mathbf{R}_{sx}\mathbf{R}_{xx}^{-1}\mathbf{R}_{sx}^{\rm H}\\ &= \mathbf{R}_{ss} - \mathbf{R}_{ss}\mathbf{H}^{\rm H}(\mathbf{H}\mathbf{R}_{ss}\mathbf{H}^{\rm H} + \mathbf{R}_{nn})^{-1}\mathbf{H}\mathbf{R}_{ss}\\ &= (\mathbf{R}_{ss}^{-1} + \mathbf{H}^{\rm H}\mathbf{R}_{nn}^{-1}\mathbf{H})^{-1}. \qquad (28)\end{aligned}$$

[5] $\mathbf{A}^{-1} - \mathbf{A}^{-1}\mathbf{B}[\mathbf{D}\mathbf{A}^{-1}\mathbf{B} + \mathbf{C}^{-1}]^{-1}\mathbf{D}\mathbf{A}^{-1} = (\mathbf{A} + \mathbf{B}\mathbf{C}\mathbf{D})^{-1}$.

[6] The maximization of the SNR is not necessarily the optimum criterion, since the MSE solution contains a bias [8,14]. Alternatively, an unbiased criterion can be found by minimizing the bit error probability.

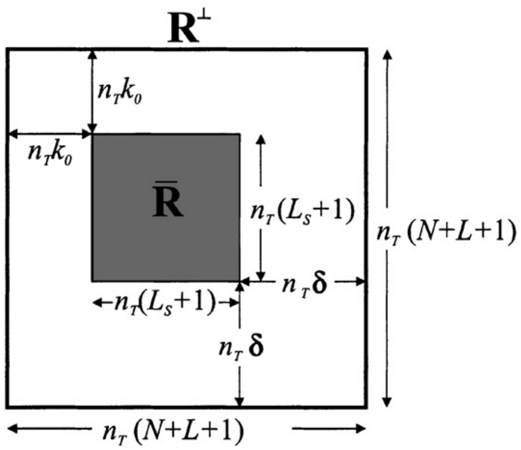

Fig. 4. Graphic interpretation of submatrix $\bar{\mathbf{R}}$ of $\mathbf{R}^{\perp}$ in dependence of delay k_0 and TIR order L_S.

It is worth to note that $\mathbf{R}^{\perp}$ does not depend on k_0 or L_S, so it needs to be computed only once for maximizing the $\mathrm{SNR}_{\mathrm{ISF}}$. The error-auto-correlation in (27) is reformulated using the definition $\tilde{\mathbf{B}} = \mathbf{B}\mathbf{\Delta}_{k_0}$ from (21)

$$\mathbf{R}_{ee} = \tilde{\mathbf{B}}\mathbf{R}^{\perp}\tilde{\mathbf{B}}^{\mathrm{H}} = \tilde{\mathbf{B}}\mathbf{\Delta}_{k_0}\mathbf{R}^{\perp}\mathbf{\Delta}_{k_0}^{\mathrm{H}}\mathbf{B}^{\mathrm{H}}$$
$$= \mathbf{B}\bar{\mathbf{R}}\mathbf{B}^{\mathrm{H}} \tag{29}$$

with $\bar{\mathbf{R}} = \mathbf{\Delta}_{k_0}\mathbf{R}^{\perp}\mathbf{\Delta}_{k_0}^{\mathrm{H}}$ being a $n_{\mathrm{T}}(L_S+1) \times n_{\mathrm{T}}(L_S+1)$ submatrix of $\mathbf{R}^{\perp}$ parameterized by k_0 and L_S. The upper left element of $\bar{\mathbf{R}}$ corresponds to the (k_0+1)th diagonal element of $\mathbf{R}^{\perp}$, and the size of $\bar{\mathbf{R}}$ is determined by L_S. A graphic interpretation of this submatrix in dependence of the delay parameter k_0 and TIR order L_S is shown in Fig. 4 for a given number of transmit antennas n_{T}, filter order N, and channel order L.

3.3. Shortening concepts and equalization strategies

In this section, different constraints for solving the optimization problem (25) are proposed. First, the optimum shortening algorithm in the sense of minimizing the trace $(\mathbf{R}_{ee})$ is introduced (called ONC). This is the best solution, when the main task is to shorten a MIMO channel [1]. As long as the target system remains frequency-selective ($L_S > 0$), additional space-time equalizing techniques or the use of MIMO-OFDM are necessary to detect the transmitted signals. For the special case of a non-frequency-selective target system ($L_S = 0$) we propose an easy detection scheme, being a kind of a linear detection equalizer.

In addition to this optimum shortening algorithm, two other constraints are presented (called ITC and MLTC). These constraints directly allow a detection of the transmitted signals by MIMO decision feedback equalization (MIMO-DFE).

3.3.1. Orthogonality constraint (ONC)

Under the ONC, the target system $\mathbf{B}$ is constrained to have orthogonal rows, i.e., $\mathbf{B}\mathbf{B}^{\mathrm{H}} = I_{n_S}$. With this constraint the average energy of all layers at the output of the ISF $\mathbf{W}$ are equal. Using the ordered eigendecomposition of the $n_{\mathrm{T}}(L_S+1) \times n_{\mathrm{T}}(L_S+1)$ submatrix $\bar{\mathrm{R}}$ [7]

$$\bar{\mathbf{R}} = \mathbf{U}\mathbf{\Lambda}\mathbf{U}^{\mathrm{H}} = \mathbf{U}\,\mathrm{diag}(\lambda_1,\ldots,\lambda_{n_{\mathrm{T}}(L_S+1)})\mathbf{U}^{\mathrm{H}} \tag{30}$$

with $\lambda_1 \leqslant \lambda_2 \leqslant \cdots \leqslant \lambda_{n_{\mathrm{T}}(L_S+1)}$, the error-auto-correlation (29) becomes

$$\mathbf{R}_{ee} = \mathbf{B}\bar{\mathbf{R}}\mathbf{B}^{\mathrm{H}} = \mathbf{B}\mathbf{U}\mathbf{\Lambda}\mathbf{U}^{\mathrm{H}}\mathbf{B}^{\mathrm{H}}. \tag{31}$$

The equalizer output SNR is maximized (correspondingly, the trace of $\mathbf{R}_{ee}$ is minimized) in the case of $\mathbf{R}_{ee}$ being a diagonal matrix [4], which results in the condition

$$\mathbf{B}\mathbf{U} = [\mathbf{I}_{n_S} \quad \mathbf{0}_{n_S \times n_{\mathrm{T}}(L_S+1)-n_S}] \tag{32}$$

and consequently the optimum TIR and the error-autocorrelation are given by

$$\mathbf{B}_{\mathrm{opt}}^{\mathrm{ONC}} = [\mathbf{I}_{n_S} \quad \mathbf{0}_{n_S \times n_{\mathrm{T}}(L_S+1)-n_S}]\mathbf{U}^{\mathrm{H}} \tag{33}$$

$$\mathbf{R}_{ee,\min}^{\mathrm{ONC}} = \mathrm{diag}(\lambda_1,\ldots,\lambda_{n_S}). \tag{34}$$

As $\bar{\mathbf{R}}$ has $n_{\mathrm{T}}(L_S+1)$ eigenvalues, the number of receive antennas n_S of the target system $\mathbf{B}$ is limited by $n_S \leqslant n_{\mathrm{T}}(L_S+1)$ and allowing $n_S > n_{\mathrm{T}}$ may be used to achieve an additional diversity gain depending on the regarded MIMO transmission scheme and the applied detection strategie [5].

As already mentioned, reducing the impulse length with ONC filtering requires an additional equalization step for signal detection or the application of MIMO-OFDM, in general. Nevertheless, a non-frequency-selective TIR is achieved [8] by setting

[7] $\mathrm{diag}(\lambda_1,\ldots,\lambda_\alpha)$ denotes a $\alpha \times \alpha$ diagonal matrix with the diagonal elements $\lambda_1,\ldots,\lambda_\alpha$.

[8] By equalizing the FS-MIMO system to a non-frequency-selective system $\mathbf{B}$ with $L_S = 0$ the maximum number of equivalent receive antennas n_S is limited by $n_S \leqslant n_{\mathrm{T}}(L_S+1) = n_{\mathrm{T}}$.

$L_S = 0$ and to detect the layers of such a truncated MIMO system, the well known V-BLAST algorithm could be applied [22]. It generally detects the distinct layers by a successive interference cancellation technique which nulls the interferer by linearly weighting the received signal vector with a zero-forcing nulling vector. By taking into account that $\mathbf{B}$ is a $n_T \times n_T$ unitary matrix $\mathbf{B}\mathbf{B}^H = \mathbf{B}^H\mathbf{B} = \mathbf{I}_{n_T}$ the V-BLAST scheme simplifies, as the layers are already separated in space and consequently the interference cancellation step can be omitted. Using (19) with $\mathbf{W}\underline{\mathbf{x}}(k) = \mathbf{B}\underline{\tilde{\mathbf{s}}}(k-k_0) - \mathbf{e}(k)$, the ISF output in (14) becomes

$$\mathbf{y}(k) = \mathbf{W}\underline{\mathbf{x}}(k) = \mathbf{B}\underline{\tilde{\mathbf{s}}}(k-k_0) - \mathbf{e}(k). \tag{35}$$

By multiplying the ISF output (35) with $\mathbf{B}^H$ and considering $\underline{\tilde{\mathbf{s}}}(k-k_0) = \mathbf{s}(k-k_0)$ for $L_S = 0$ a modified received vector $\mathbf{z}(k) = [z_1(k), \ldots, z_{n_T}(k)]^T$ is achieved

$$\begin{aligned}\mathbf{z}(k) &= \mathbf{B}^H\mathbf{y}(k)\\ &= \mathbf{B}^H\mathbf{B}\underline{\tilde{\mathbf{s}}}(k-k_0) + \mathbf{B}^H\mathbf{e}(k)\\ &= \mathbf{s}(k-k_0) + \check{\mathbf{n}}(k),\end{aligned} \tag{36}$$

with $\check{\mathbf{n}}(k)$ denoting a modified noise vector. The modified received vector $\mathbf{z}(k)$ contains no ISI nor ILI, but denotes an immediate measurement for transmit signal $\mathbf{s}(k-k_0)$. Consequently, the transmitted layers can easily be detected by applying an appropriate quantization function to the elements of this modified received vector. Summarizing this scheme, it yields an equalization in space and time domain and can therefore be regarded as a linear equalizer.

3.3.2. *Tap constraint (TC)*

Under the tap constraint (TC), one matrix tap $\mathbf{B}(v)(0 \leqslant v \leqslant L_S)$ of the TIR $\mathbf{B}$ is forced to be equal to a determined matrix $\mathbf{C}$ of dimension $n_T \times n_T$, which immediately implies $n_S = n_T$. Therefore the optimization problem (25) was solved in [4] with respect to the constraint $\mathbf{B}\mathbf{\Phi} = \mathbf{C}$ using the definitions [9]

$$\mathbf{\Phi} = \begin{bmatrix} \mathbf{0}_{vn_T \times n_T} \\ \mathbf{I}_{n_T} \\ \mathbf{0}_{(L_S - v)n_T \times n_T} \end{bmatrix}. \tag{37}$$

The solution of this problem is given by

$$\mathbf{B}^{TC}_{opt} = \mathbf{C}(\mathbf{\Phi}^H\bar{\mathbf{R}}^{-1}\mathbf{\Phi})^{-1}\mathbf{\Phi}^H\bar{\mathbf{R}}^{-1} \tag{38}$$

$$\mathbf{R}^{TC}_{ee,\min} = \mathbf{C}(\mathbf{\Phi}^H\bar{\mathbf{R}}^{-1}\mathbf{\Phi})^{-1}\mathbf{C}. \tag{39}$$

To achieve not only an impulse shortening, but also a scheme for detecting FS-MIMO systems, we further specify this solution of the optimization problem (25) by applying the tap constraint to the first matrix tap of $\mathbf{B}$, i.e., $v = 0$, or more specifically, $\mathbf{B}(0) = \mathbf{C}$. As we shall see later on, this restriction allows efficient MIMO-DFE structures. For the special case of $v = 0$, (37) becomes $\mathbf{\Phi} = [\mathbf{I}_{n_T} \ \ \mathbf{0}_{n_T \times n_T L_S}]^T$ and with using the partition [10]

$$\bar{\mathbf{R}}^{-1} = \begin{bmatrix} \mathbf{R}_{11} & \mathbf{R}_{12} \\ \mathbf{R}_{12}^H & \mathbf{R}_{22} \end{bmatrix} \tag{40}$$

the TIR structure can be viewed in detail. With these definitions (38) becomes

$$\begin{aligned}\mathbf{B}^{TC}_{opt,v=0} &= \mathbf{C}(\mathbf{\Phi}^H\bar{\mathbf{R}}^{-1}\mathbf{\Phi})^{-1}\mathbf{\Phi}^H\bar{\mathbf{R}}^{-1}\\ &= \mathbf{C}\mathbf{R}_{11}^{-1}[\mathbf{R}_{11} \quad \mathbf{R}_{12}]\\ &= \mathbf{C}[\mathbf{I}_{n_T} \quad \mathbf{R}_{11}^{-1}\mathbf{R}_{12}]\end{aligned} \tag{41}$$

and the error-autocorrelation (39) simplifies as

$$\begin{aligned}\mathbf{R}^{TC}_{ee,\min,v=0} &= \mathbf{C}(\mathbf{\Phi}^H\bar{\mathbf{R}}^{-1}\mathbf{\Phi})^{-1}\mathbf{C}\\ &= \mathbf{C}\mathbf{R}_{11}^{-1}\mathbf{C}.\end{aligned} \tag{42}$$

These equations indicate the general solution of the optimization problem, when restricting $\mathbf{B}(0)$ to be equal to a defined matrix $\mathbf{C}$. In this case, the output of the ISF filter is given by

$$\begin{aligned}\mathbf{y}(k) &= \mathbf{C}\mathbf{s}(k-k_0) + \sum_{l=1}^{L_S}\mathbf{B}(l)\mathbf{s}(k-k_0-l) + \check{\mathbf{n}}(k)\\ &= \mathbf{C}\mathbf{s}(k-k_0) + \sum_{l=1}^{L_S}\mathbf{B}(l)\hat{\mathbf{s}}(k-k_0-l) + \check{\mathbf{n}}(k)\\ &= \mathbf{C}\mathbf{s}(k-k_0) + \hat{\mathbf{d}}(k) + \check{\mathbf{n}}(k)\end{aligned} \tag{43}$$

with $\hat{\mathbf{d}}(k)$ denoting the interference of previously transmitted signals assuming correct previous decisions ($\hat{\mathbf{s}}(k-k_0-l) = \mathbf{s}(k-k_0-l)$ for $1 \leqslant l \leqslant L_S$) and

[9] With $\mathbf{B}\mathbf{\Phi}$, matrix tap v of $\mathbf{B}$ is highlighted and the remaining taps are cancelled.

[10] Matrix $\mathbf{R}_{11}$ is of dimension $n_T \times n_T$.

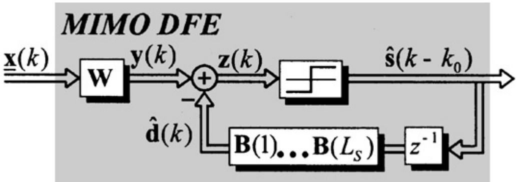

Fig. 5. Block diagram of the MIMO decision feedback equalizer.

$\check{\mathbf{n}}(k)$ indicating a modified noise vector. Subtracting the estimated interference from the filter output

$$\mathbf{z}(k) = \mathbf{y}(k) - \hat{\mathbf{d}}(k) = \mathbf{C}\mathbf{s}(k-k_0) + \check{\mathbf{n}}(k), \tag{44}$$

a direct measurement $\mathbf{z}(k)$ for the transmit signals $\mathbf{s}(k-k_0)$ is achieved, which can be detected utilizing an appropriate scheme according to the chosen constraint matrix $\mathbf{C}$. Hence, the influence of previously decisions are subtracted from the filter output, a MIMO-DFE [11] structure is achieved, as shown in Fig. 5.

In the special case of a non-frequency-selective TIR, i.e. by setting $L_S = 0$, a linear equalizer (LE) in time direction is already achieved by the impulse shortening filter. Consequently, the MIMO-DFE structure simplifies to a memoryless detector and the signals are detected according to the structure of $\mathbf{C}$.

Depending on the chosen constraint $\mathbf{C}$, appropriate schemes for detecting the transmitted signals $\mathbf{s}(k-k_0)$ on basis of $\mathbf{z}(k)$ have to be selected. In the sequel, we will introduce two common constraints, specify the solution of the optimization problem, and propose corresponding detection schemes.

3.3.2.1. Identity tap constraint (ITC) The identity tap constraint (ITC) chooses $\mathbf{C}$ to be equal to the identity matrix, i.e., $\mathbf{C} = \mathbf{I}_{n_T} = \mathbf{B}(0)$. With this condition, the ISF output (43) gets

$$\mathbf{y}(k) = \mathbf{s}(k-k_0) + \hat{\mathbf{d}}(k) + \check{\mathbf{n}}(k) \tag{45}$$

and the detector input vector becomes

$$\mathbf{z}(k) = \mathbf{y}(k) - \hat{\mathbf{d}}(k) = \mathbf{s}(k-k_0) + \check{\mathbf{n}}(k). \tag{46}$$

This vector directly denotes a value to independently estimate the signals $\mathbf{s}(k-k_0)$, hence the signals are separated in space-domain. Using the restriction $\mathbf{C} = \mathbf{I}_{n_T}$ in (41) and (42) the TIR and the error-autocorrelation becomes

$$\mathbf{B}_{\text{opt}}^{\text{MMSE-DFE}} = [\mathbf{I}_{n_T} \quad \mathbf{R}_{11}^{-1}\mathbf{R}_{12}], \tag{47}$$

$$\mathbf{R}_{ee,\min}^{\text{MMSE-DFE}} = \mathbf{R}_{11}^{-1}, \tag{48}$$

respectively, which correspond to the MIMO MMSE-DFE structure studied in [3].

By determining $L_S = 0$ a non-frequency-selective TIR is achieved and the TIR is obviously given by

$$\mathbf{B}_{\text{opt}}^{\text{LE}} = \mathbf{I}_{n_T}. \tag{49}$$

Thus a full equalization in space and time domain is achieved by the impulse shortening filter, which implies a direct detection of the distinct layers. It is worth to note that this linear equalization scheme and the linear equalization scheme for ONC shortening proposed in Section 3.3.1 obtain the same bit error rate performance as both methods perform a full equalization in space–time-domain.

3.3.2.2. Monic lower triangular constraint (MLTC) Instead of using the ITC condition, we now restrict $\mathbf{C} = \mathbf{B}(0)$ to be a monic [12] lower triangular matrix. With the Cholesky factorization $\mathbf{R}_{11} = \mathbf{L}\mathbf{D}\mathbf{L}^{\text{H}}$, where $\mathbf{L}$ is a monic lower triangular matrix and $\mathbf{D}$ is a diagonal matrix, the error autocorrelation (42) becomes

$$\mathbf{R}_{ee,\min,v=0}^{\text{TC}} = \mathbf{C}\mathbf{R}_{11}^{-1}\mathbf{C} = \mathbf{C}\mathbf{L}^{-\text{H}}\mathbf{D}^{-1}\mathbf{L}^{-1}\mathbf{C}. \tag{50}$$

The optimum monic lower triangular matrix $\mathbf{C} = \mathbf{B}(0)$ that minimizes trace of (50) is given by the matrix $\mathbf{B}(0) = \mathbf{L}$ [4]. With this definition, the TIR and the error-autocorrelation becomes

$$\mathbf{B}_{\text{opt}}^{\text{MLTC}} = [\mathbf{L} \quad \mathbf{D}^{-1}\mathbf{L}^{-1}\mathbf{R}_{12}] \tag{51}$$

$$\mathbf{R}_{ee,\min}^{\text{MLTC}} = \mathbf{D}^{-1}, \tag{52}$$

respectively. For MLTC the filter output signal in (43) specifies as

$$\mathbf{y}(k) = \mathbf{L}\mathbf{s}(k-k_0) + \hat{\mathbf{d}}(k) + \check{\mathbf{n}}(k) \tag{53}$$

and an ISI-free signal can again be achieved by subtracting the estimated interference in a MIMO-DFE structure. Under the assumption of correct previous decisions this detector input signal (44) gets

$$\mathbf{z}(k) = \mathbf{L}\mathbf{s}(k-k_0) + \check{\mathbf{n}}(k). \tag{54}$$

[11] In the context of CDMA an equivalent *matrix* DFE applying infinite impulse response filter has been proposed in [10].

[12] A monic matrix has diagonal elements equal to one.

Table 1
Overview of target impulse responses for ONC, ITC, and MLTC constraint and appropriate detection schemes for different TIR order L_S

Const.	L_S	$\mathbf{B} = [\mathbf{B}(0) \ldots \mathbf{B}(L_S)]$	Comment
ONC	> 0		OFDM
	$= 0$	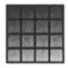	LE
ITC	> 0		DFE
	$= 0$		LE
MLTC	> 0		DFE
	$= 0$		SIC

Hence, $\mathbf{L}$ is a lower triangular matrix, $\mathbf{z}(k)$ is partly free from ILI and can be detected by a successive interference cancellation (SIC) technique, which executes a decision feedback equalization in space direction. This method is similar to the detection of non-frequency selective V-BLAST systems using the QR decomposition of the channel matrix [23,24]. The only difference concerns the order of detection, which is from top to bottom [13] due to $\mathbf{L}$ being lower triangular. By restricting $L_S = 0$ under MLTC condition the MIMO-DFE structure simplifies again to a memoryless detector and the signals can directly be detected using the SIC scheme.

3.3.3. Survey of the detection schemes

As an overview, Table 1 summarizes the different impulse shortening and equalization schemes discussed so far. For the different constraints, it graphically shows the resulting target systems $\mathbf{B}$ for a TIR order of $L_S > 0$ and $L_S = 0$. Comments about appropriate detection schemes are given in the last column.

It was shown in [1] that ONC impulse shortening always outperforms ITC in sense of maximizing the $\mathrm{SNR}_{\mathrm{ISF}}$. Therefore it is the best solution for reducing the number of effective taps. In general, additional space–time equalization techniques like MIMO-OFDM or frequency-domain equalization are necessary for signal detection. In the special case of a non-frequency-selective target system, a memory less detector can be applied.

The ITC and the MLTC shortening algorithms are a special case of the more general tap constraint. By restricting the first tap of the target system to specific values, both schemes can be used in a MIMO-DFE structure. In case of ITC, the first tap is forced to an identity matrix, which achieves a separation in space–domain for the according transmit signal. By subtracting previously detected signals from the filter output a modified signal that is free from ISI and ILI is obtained, which can be decided by an appropriate quantization function. For $L_S = 0$ a complete separation in space–time-domain is achieved and the signal can be detected directly.

In contrast to ITC the second approach MLTC achieves only a partly separation in space-domain and requires a successive interference cancellation technique in addition to the MIMO-DFE structure. For the specific case of a non-frequency-selective target system the transmit signals can directly be detected by using a SIC detector. In [4] it was shown, that MLTC outperforms ITC in sense of $\mathrm{SNR}_{\mathrm{ISF}}$ and additionally, efficient schemes optimizing the decision delay k_0 have been discussed.

3.4. Simulation results

In the sequel, we investigate the bit error rate (BER) for a frequency-selective MIMO system with $n_T = 4$, $n_R = 6$ antennas and uncoded QPSK modulation. E_b denotes the average energy per information bit arriving at the receiver, thus $\sigma_s^2 = \log_2(M)E_b/n_R$ holds. For a varying channel order L, Fig. 6 shows the BER of ONC impulse shortening with filter order $N = 10$ and linear equalization according to (36). As a reference, the BER of V-BLAST for a non-frequency-selective MIMO channel ($L = 0$) is included.

The BER performance becomes worse with an increasing number of matrix taps L due to an increasing MSE. Shortening a channel of order $L = 6$ to

[13] Consequently, the sequence of detection is given by $s_1(k-k_0), s_2(k-k_0), \ldots, s_{n_T}(k-k_0)$.

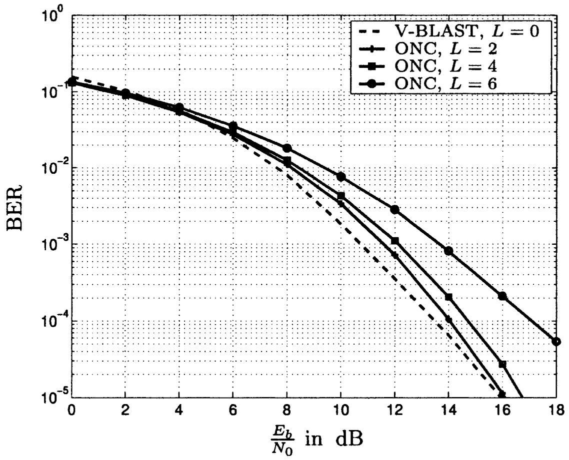

Fig. 6. ONC shortening with filter order $N=10$ and linear equalization for a varying MIMO channel order L.

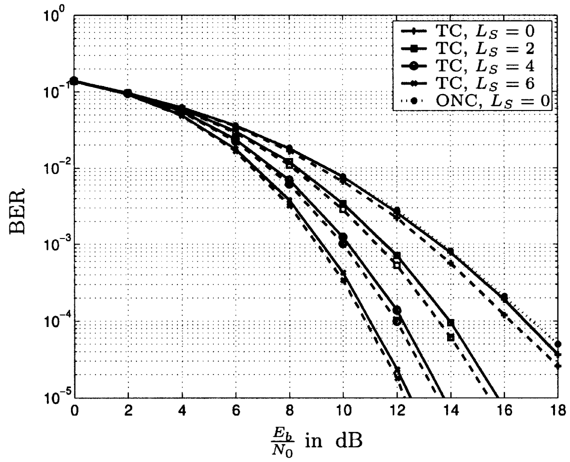

Fig. 8. ITC (solid lines) and MLTC (dotted lines) equalization of a frequency-selective channel of order $L=6$, filter order $N=10$ and varying TIR order $L_{\rm S}$. ONC with $L_{\rm S}=0$ and memoryless detector is denoted by dots.

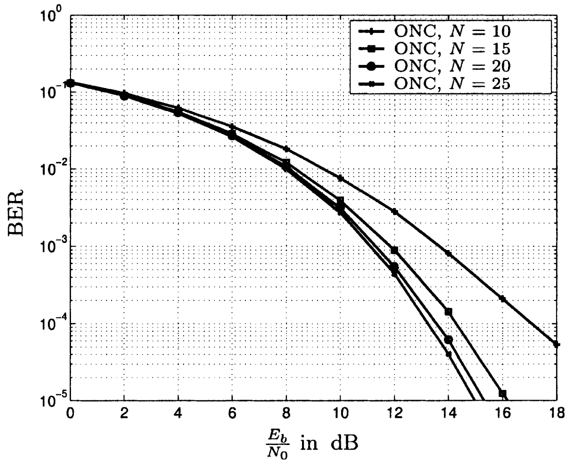

Fig. 7. ONC shortening and linear equalization of a frequency-selective MIMO channel of order $L=6$ with varying ISF order N.

a non-frequency-selective target system results in a number of pre and post taps not neglected by the TIR, which results in a remaining ISI and effects a noise enhancement.

For the same receiver structure, the BER performance for a MIMO system with channel order $L=6$ and varying filter order N is shown in Fig. 7. As expected, increasing the number of filter taps N results in an improved performance but on the expense of an increased computational complexity. The improvement of the $\mathrm{SNR}_{\mathrm{ISF}}$ with increasing N has been investigated in [1] and shows, that the $\mathrm{SNR}_{\mathrm{ISF}}$ converges to a determined value. Consequently, incrementing the filter order above $N=25$ will only lead to a small BER improvement for this example.

The performance of the decision feedback structures ITC and MLTC, including the special case of linear equalization by $L_{\rm S}=0$, is discussed next. For a channel order $L=6$ and filter order $N=10$, Fig. 8 shows the BER for ITC and MLTC impulse shortening with varying TIR order $L_{\rm S}$ and appropriate decision feedback structure. The performance of ONC with $L_{\rm S}=0$ and memoryless detection corresponds to ITC with $L_{\rm S}=0$, since both schemes perform linear equalization. It is obvious that MLTC outperforms ITC for every configuration due to the higher equalizer SNR. Furthermore, the noise enhancement reduces with an increasing TIR order $L_{\rm S}$ and therefore results in a better BER.

4. Frequency selective BLAST

4.1. Principle of FS-BLAST

In this section, we investigate the frequency selective extension of V-BLAST as proposed in [16,17] and

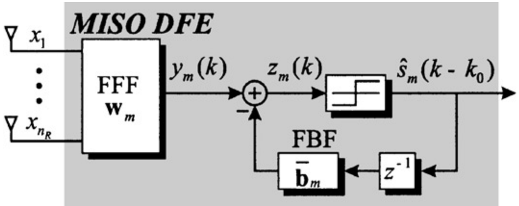

Fig. 9. Initial MISO-DFE stage of FS-BLAST to detect layer m.

call it FS-BLAST. Similar to V-BLAST, in each detection step one layer is treated as target layer and all other layers are treated as interferers. The target layer is detected by suppressing the inter-layer interferers, the estimated signals are subtracted from the received signal; the remaining layers are detected in the same successive way.

To derive the receiver structure, we use the DFE structure consisting of a MISO feedforward filter (FFF) and a SISO feedbackward filter (FBF) shown in Fig. 9. It is worth to note that this DFE structure is only used for filter derivation, whereas in the implementation *near* MLSE equalizer may be used in each stage, as explained in Section 4.3.

The sequence of received signals is again filtered in space and time domain, but the aim of this FFF is now to extract the target layer m, but suppress the other layers and also part of the own ISI. The FBF filters the sequence of decisions on previously detected symbols delayed by k_0 time steps and its output is subtracted from the FFF output. Thus, the feedbackward filter is used to remove that part of ISI from the present estimate caused by previously detected symbols.

4.2. MISO-filter design

To calculate the FFF and the FBF, the MISO model defined in Section 2.3 is adopted. The main reason for using this model is the signal alignment of each target layer m in a sequence, as given by (6). To define the FFF and the FBF, the input–output relation in (7) has to be extended to describe a *sequence* of received signals. To calculate the sequence vector $\underline{\mathbf{x}}(k)$ (defined in (8) to denote a sequence of $N+1$ received signals) the transmit signal vector (6) is extended to the $(N+L+1)\times 1$ sequence vector

$$\bar{\mathbf{s}}_m(k) = \begin{bmatrix} s_m(k) \\ \vdots \\ s_m(k-L-N) \end{bmatrix}. \tag{55}$$

By utilizing the $n_R(N+1)\times(N+L+1)$ block Toeplitz matrix [14]

$$\bar{\mathbf{H}}_m = \begin{bmatrix} \boxed{\mathbf{H}_m} & & & \\ & \boxed{\mathbf{H}_m} & & \\ & & \ddots & \\ & & & \boxed{\mathbf{H}_m} \end{bmatrix}, \tag{56}$$

the input–output relation for a sequence of received signals is given by

$$\underline{\mathbf{x}}(k) = \sum_{m=1}^{n_T} \bar{\mathbf{H}}_m \bar{\mathbf{s}}_m(k) + \underline{\mathbf{n}}(k). \tag{57}$$

At the first stage of detection, the sequence of received signals $\underline{\mathbf{x}}(k)$ is filtered by the MISO FFF $\mathbf{w}_m$ and the filter output (14) becomes

$$y_m(k) = \sum_{l=0}^{N} \mathbf{w}_m(l)\mathbf{x}(k-l) = \mathbf{w}_m \underline{\mathbf{x}}(k). \tag{58}$$

In contrast to the ISF used in Section 3, the FFF $\mathbf{w}_m$ has only one output signal and by using a small letter the filter is indicated to be a vector. Consequently, the row vector [15] $\mathbf{w}_m = [\mathbf{w}_m(0)\ \ \mathbf{w}_m(1)\ \ \ldots\ \ \mathbf{w}_m(N)]$ of dimension $1\times n_R(N+1)$ denotes the FFF and consists of

[14] By describing column l of matrix $\mathbf{H}_m$ by vector $(\mathbf{H}_m)_l$ the channel matrix is given $\mathbf{H}_m = [(\mathbf{H}_m)_1\ \ (\mathbf{H}_m)_2\ \ \ldots\ \ (\mathbf{H}_m)_{L+1}]$ and (56) reads

$$\bar{\mathbf{H}}_m = \begin{bmatrix} (\mathbf{H}_m)_1 & (\mathbf{H}_m)_2 & \cdots & 0 & \\ 0 & (\mathbf{H}_m)_1 & \cdots & (\mathbf{H}_m)_{L+1} & \\ 0 & 0 & \ddots & \ddots & \ddots \end{bmatrix}$$

and is block Toeplitz.

[15] With respect to Section 3 vector $\mathbf{w}_m$ can be regarded as one row of an impulse shortening filter matrix $\mathbf{W}$. In contrast to ISF the feedforward filter is only derived with respect to one layer m and the calculation of the remaining FFF bases on a stepwise reduced channel matrix as remarked later on.

$N+1$ space-only filter taps $\mathbf{w}_m(l) = [w_{m,1}(l) \; \dots \; w_{m,n_\mathrm{R}}(l)]$ each of dimension $1 \times n_\mathrm{R}$.

To get an ISI-free representation for $s_m(k-k_0)$, the sequence of L_S most recent decisions of target layer m

$$\hat{\mathbf{s}}_m(k-k_0-1) = \begin{bmatrix} \hat{\mathbf{s}}_m(k-k_0-1) \\ \vdots \\ \hat{\mathbf{s}}_m(k-k_0-L_\mathrm{S}) \end{bmatrix} \quad (59)$$

is filtered by the $1 \times L_\mathrm{S}$ feedbackward filter [16] (FBF) $\bar{\mathbf{b}}_m = [b_m(1) \; b_m(2) \; \dots \; b_m(L_\mathrm{S})]$ with decision delay k_0 to be optimized. Finally, the output of the FBF is subtracted from the FFF output

$$\begin{aligned} z_m(k) &= \mathbf{w}_m \underline{\mathbf{x}}(k) - \bar{\mathbf{b}}_m \hat{\mathbf{s}}_m(k-k_0-1) \\ &= [\mathbf{w}_m \quad \bar{\mathbf{b}}_m] \cdot \begin{bmatrix} \underline{\mathbf{x}}(k) \\ -\hat{\mathbf{s}}_m(k-k_0-1) \end{bmatrix} \\ &= \mathbf{f}_m \mathbf{a}_m \end{aligned} \quad (60)$$

and decided by utilizing an appropriate quantization device to form the estimation $\hat{s}_m(k-k_0)$ (see Fig. 9). In Eq. (60), the $1 \times n_\mathrm{R}(N+1)+L_\mathrm{S}$ row vector $\mathbf{f}_m = [\mathbf{w}_m \;\; \bar{\mathbf{b}}_m]$ contains the FFF and FBF coefficients for layer m, whereas $\mathbf{a}_m$ denotes the currently received sequence and (under the assumption of correct previous decisions $\hat{\mathbf{s}}_m(k) = \mathbf{s}_m(k)$) the negative of the transmitted sequence from antenna m delayed by k_0 taps. The MMSE solution for the filter design is found by minimizing the cost-function [17]

$$\begin{aligned} J_\mathrm{MSE} &= E\{|z_m(k) - s_m(k-k_0)|^2\} \\ &= E\{|\mathbf{f}_m \mathbf{a}_m - s_m(k-k_0)|^2\} \\ &= \mathbf{f}_m \mathbf{Q}_m \mathbf{f}_m^\mathrm{H} - \mathbf{f}_m \mathbf{p}_m - \mathbf{p}_m^\mathrm{H} \mathbf{f}_m^\mathrm{H} + \sigma_s^2 \end{aligned} \quad (61)$$

with the $n_\mathrm{R}(N+1)+L_\mathrm{S} \times 1$ vector [17]

$$\mathbf{p}_m = E\{\mathbf{a}_m s_m^*(k-k_0)\} = \sigma_s^2 \begin{bmatrix} (\bar{\mathbf{H}}_m)_{k_0+1} \\ \mathbf{0}_{N+L+1} \end{bmatrix} \quad (62)$$

and the $n_\mathrm{R}(N+1)+L_\mathrm{S} \times n_\mathrm{R}(N+1)+L_\mathrm{S}$ matrix

$$\mathbf{Q}_m = E\{\mathbf{a}_m \mathbf{a}_m^\mathrm{H}\} = \begin{bmatrix} \mathbf{R}_{xx} & -\mathbf{R}_{s_m x}^\mathrm{H} \\ -\mathbf{R}_{s_m x} & \mathbf{R}_{s_m s_m} \end{bmatrix}. \quad (63)$$

[16] We denote the filter vector by an overlined letter, to indicate it length being L_S and not $L_\mathrm{S}+1$.

[17] $(\bar{\mathbf{H}})_\alpha$ denotes column α of matrix $\bar{\mathbf{H}}$.

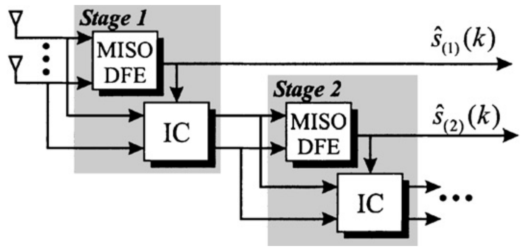

Fig. 10. First two MISO-DFE stages of the successive interference suppression and cancellation structure.

The $n_\mathrm{R}(N+1) \times n_\mathrm{R}(N+1)$ covariance matrix $\mathbf{R}_{xx}$ in (63) has already been defined in (13). The cross correlation between transmit signal $\mathbf{s}_m(k-k_0-1)$ and receive sequence $\underline{\mathbf{x}}(k)$ is calculated by

$$\begin{aligned} \mathbf{R}_{s_m x} &= E\{\hat{\mathbf{s}}_m(k-k_0-1)\underline{\mathbf{x}}^\mathrm{H}(k)\} \\ &= \sigma_s^2 (\bar{\mathbf{H}}_m)^\mathrm{H}_{k_0+2 \dots k_0+L_\mathrm{S}+1} \end{aligned} \quad (64)$$

and for the $L_\mathrm{S} \times L_\mathrm{S}$ input autocorrelation matrix we find

$$\mathbf{R}_{s_m s_m} = E\{\hat{\mathbf{s}}_m(k)\hat{\mathbf{s}}_m^\mathrm{H}(k)\} = \sigma_s^2 \mathbf{I}_{L_\mathrm{S}}. \quad (65)$$

By expanding the cost function in (61) to quadratic form $J_\mathrm{MSE} = (\mathbf{f}_m \mathbf{Q}_m - \mathbf{p}_m^\mathrm{H})\mathbf{Q}_m^{-1}(\mathbf{Q}_m \mathbf{f}_m^\mathrm{H} - \mathbf{p}_m) - \mathbf{p}_m^\mathrm{H}\mathbf{Q}_m^{-1}\mathbf{p}_m + \sigma_s^2$, the minimum of J_MSE is obviously donated by the filter vector $\mathbf{f}_m = \mathbf{p}_m^\mathrm{H}\mathbf{Q}_m^{-1}$ and the mean square error is given by $\mathrm{MSE}_m = \sigma_s^2 - \mathbf{p}_m^\mathrm{H}\mathbf{Q}_m^{-1}\mathbf{p}_m$.

According to [17] in each detection step μ the layer m with the smallest MSE_m is selected and detected with an optimized delay k_0 taken into account. After detecting the layer, its interference can be removed from the received signal $\mathbf{x}(k)$ similar to V-BLAST [12] and the corresponding entries in the channel matrix are cancelled. The remaining layers are detected in the same way and the output of detection stage μ, is given by $\hat{s}_{(\mu)}(k)$ (Fig. 10).

4.3. ML-detection

By regarding the MISO-DFE stage in Fig. 9 in terms of channel impulse shortening, the MISO filter creates a SISO channel of order L_S between transmit antenna m and the output $y_m(k)$ of the FFF. The target impulse response (TIR) of this SISO channel is given by the $1 \times (L_\mathrm{S}+1)$ row vector $\mathbf{b}_m = [b_m(0) \;\; \bar{\mathbf{b}}_m] = [b_m(0) \; b_m(1) \; \dots \; b_m(L_\mathrm{S})]$ and consequently a standard MLSE algorithm can be used for equalizing the

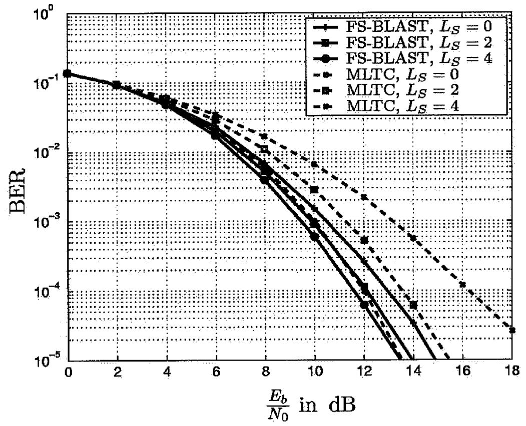

Fig. 11. BER for a frequency-selective MIMO channel of order $L = 6$ and MLTC equalization and FS-BLAST with filter order $N = 10$ for varying TIR order L_S.

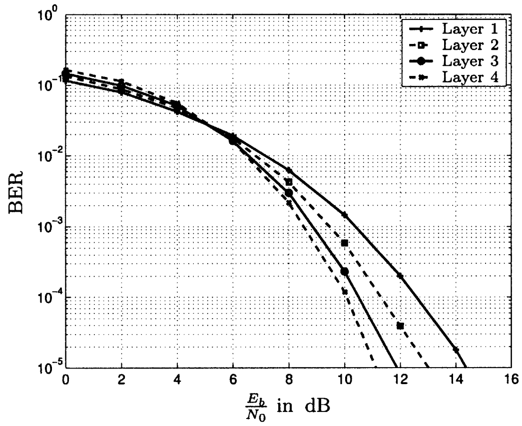

Fig. 12. BER per layer for a system with $n_T = 4$ and $n_T = 6$ antennas, QPSK modulation, frequency-selective channel of order $L = 6$, FS-BLAST with filter order $N = 10$ and TIR order $L_S = 4$.

FFF output stream with a (reduced) channel order L_S. Under ideal conditions the filter tap $b_m(0)$ should be equal to one, whereas in the presence of noise it is not. Its value is determined by [18] $b_m(0) = \mathbf{w}_m(\bar{\mathbf{H}}_m)_{k_0+1}$.

In the remainder of this section, we always assume *near* MLSE of the FFF output, which outperforms a time-domain DFE in general. Therefore, the design criteria for a FS-BLAST receiver are given by the feedforward filter order N, the decision delay k_0 and the order L_S of the target impulse response. By reducing the order L_S, the equalizer effort is decreased enormously at the expense of performance degradation.

4.4. Simulation result

To compare the performance of FS-BLAST with MLTC, we use the system described in Section 3.4 with $n_T = 4$, $n_R = 6$ antennas and QPSK modulation. Fig. 11 shows the BER for a FS-MIMO system with $L = 6$ using prefilter of order $N = 10$ and a varying TIR order L_S.

For $L_S = 0$ and 2 the FS-BLAST significantly outperforms MLTC detection due to the successive detection algorithm. With an increasing TIR order L_S the bit error rate of FS-BLAST improves as the noise enhancement reduces, but with the cost of an increasing computational complexity for MLSE detection. For a TIR order of $L_S = 4$ only a small difference between MLTC and FS-BLAST exists.

To motivate our iterative extension of FS-BLAST, Fig. 12 shows the BER for each layer in order of detection. In the lower SNR region error propagation has a large influence, hence the layer detected first performs slightly better than the layers detected in the subsequent. The BER curves traverse at a SNR of approximately 5dB, which presents the decreasing influence of error propagation. Consequently, the performance of the later detected layers improves due to their higher diversity degree. [19] Based on this observation, we propose an iterative detection scheme in the next paragraph, which is a generalization of the Backward Iterative Cancellation algorithm presented in [7].

4.5. Backward-iterative cancellation

To enhance the performance of V-BLAST, Benjebbour et al. proposed an iterative improvement of the successive detection scheme for flat fading channels [7]. In this section we apply the key note of the backward iterative cancellation (BIC) detection scheme to frequency-selective channels and therefore call it

[18] Hence $b_m(0)$ is smaller than one, the MMSE solution is biased [8] and the signal $z_m(k)$ has to be scaled by $1/b_m(0)$ prior to threshold decision in the DFE structure Fig. 9.

[19] As an example, for a flat-fading system with $n_T = 4$ and $n_R = 6$ antennas, the first layer is detected with an antenna diversity of $g_d = n_R - n_T + 1 = 3$, whereas the second layer achieves a higher diversity $g_d = n_R - (n_T - 1) + 1 = 4$ [24].

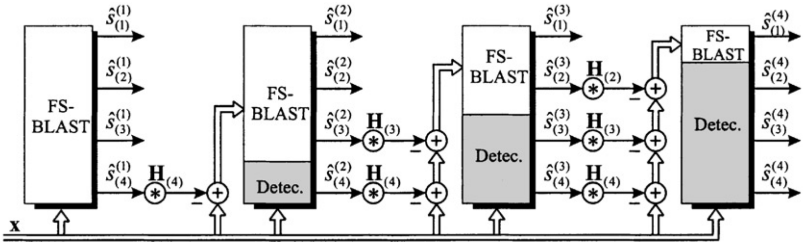

Fig. 13. Block diagram of the iterative FS-BIC detection scheme for a system with $n_T = 4$ transmit antennas with $*$ denoting the convolution.

FS-BIC. A block diagram of this algorithm for a system with $n_T = 4$ antennas is shown in Fig. 13.

In the first iteration ($i = 1$) of FS-BIC, the common FS-BLAST algorithm as proposed in Section 4.2 is applied (denoted by FS_BLAST($\mathbf{x}$)). The estimates of the first detected layer are denoted by[20] $\hat{s}^{(1)}_{(1)}$, whereas $\hat{s}^{(1)}_{(\mu)}$ is the output of stage μ. After detecting all layers with the FS-BLAST algorithm, the interference of the layer detected last ($\hat{s}^{(1)}_{(n_T)}$) is subtracted from the received signal $\mathbf{x}$ to get a modified received signal vector

$$\grave{\mathbf{x}} = \mathbf{x} - \mathbf{H}_{(n_T)} \hat{\mathbf{s}}^{(1)}_{(n_T)} \tag{66}$$

and the corresponding coefficients of the channel matrix are set to zero. The detection of the remaining $n_T - 1$ layer denoted by FS_BLAST($\grave{\mathbf{x}}$) is repeated with the FS_BLAST algorithm and the output is denoted by $\hat{s}^{(2)}_{(1)}, \ldots, \hat{s}^{(2)}_{(n_T-1)}$. To renew the detection of the high-diversity layer (n_T), the influences of these new estimates are subtracted from the receive signal $\mathbf{x}$ and by equalizing

$$\mathbf{x}_{(n_T)} = \mathbf{x} - \sum_{m=1}^{n_T-1} \mathbf{H}_{(m)} \hat{\mathbf{s}}^{(2)}_{(m)} \tag{67}$$

we obtain $\hat{s}^{(2)}_{(n_T)}$.

In the third iteration step, the interference of $\hat{s}^{(2)}_{(n_T)}$ and $\hat{s}^{(2)}_{(n_T-1)}$ is subtracted from the received signal and consequently only the first $n_T - 2$ layers are detected by FS-BLAST. With these new replicas, the estimates for layer (n_T) and ($n_T - 1$) are renewed, again. The whole iterative detection algorithm contains n_T iteration steps and is summarized in Table 2.

[20] To simplify the description, we omit the time index k in the remainder of this paragraph.

Table 2
FS-BIC Algorithm

- Initial FS_BLAST($\mathbf{x}$) of all layers to get estimates $\hat{s}^{(1)}_{(1)}, \ldots, \hat{s}^{(1)}_{(n_T)}$
- for $i = 2, \ldots, n_T$
  - Remove high diversity estimates $\hat{\mathbf{s}}^{(i-1)}_{(m)}$ from received signal $\mathbf{x}$ to achieve modified received signal for remaining layer $(1), \ldots, (n_T - i + 1)$

    $$\grave{\mathbf{x}} = \mathbf{x} - \sum_{m=n_T-(i-2)}^{n_T} \mathbf{H}_{(m)} \hat{\mathbf{s}}^{(i-1)}_{(m)}$$
  - Apply FS_BLAST($\grave{\mathbf{x}}$) to renew estimates $\hat{s}^{(i)}_{(1)}, \ldots, \hat{s}^{(i)}_{(n_T-i+1)}$
  - for $\mu = n_T - (i-2), \ldots, n_T$
    - · To improve detection of layer (μ), remove renewed estimates of lower diversity layers and past estimates of higher diversity layers

      $$\mathbf{x}_\mu = \mathbf{x} - \sum_{m=1}^{\mu-1} \mathbf{H}_{(m)} \hat{\mathbf{s}}^{(i)}_{(m)} - \sum_{m=\mu+1}^{n_T} \mathbf{H}_{(m)} \hat{\mathbf{s}}^{(i-1)}_{(m)}$$
    - · Equalize $\mathbf{x}_\mu$ to achieve estimate $\hat{s}^{(i)}_{(\mu)}$
  - end
- end

4.6. Performance of FS-BIC

In this section we investigate the performance of the iterative FS-BIC algorithm for the system determined

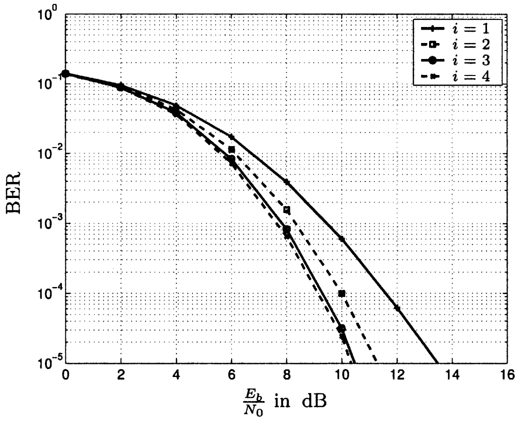

Fig. 14. BER versus iteration number i for channel order $L = 6$, FFF order $N = 10$ and target impulse response (TIR) order $L_S = 4$.

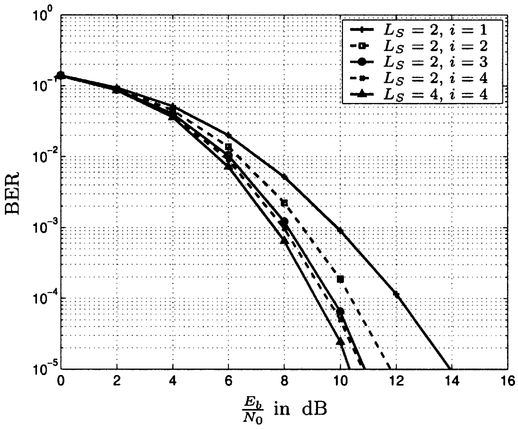

Fig. 15. BER versus iteration number i for FS-BLAST with TIR order $L_S = 2$ and 4.

in Section 4.4 with $n_T = 4$ and $n_R = 6$ antennas, QPSK modulation, channel order of $L = 6$ and FFF order of $N = 10$. Fig. 14 shows the BER in each iteration for a receiver with a TIR order of $L_S = 4$. An improvement of about 2.3 dB is visible for the second iteration step compared to the initial detection stage. The improvement in the third iteration becomes smaller, but is still remarkable, whereas the fourth iteration leads only to a slight enhancement.

Fig. 15 shows the BER versus number of iteration for the same system, but with a TIR order of only $L_S = 2$, which results in a decrease in computational complexity due to the smaller trellis. The performance is again improved by the iterative detection algorithm and only a difference of approximately 0.5 dB compared with the detector with $L_S = 4$ is visible for a BER of 10^{-5}.

It is worth to note that the order of detection and the corresponding decision delay k_0 from the first iteration step can be retained for the subsequent steps. Consequently, the computational effort for these iteration steps is enormously smaller compared to the first step.

5. Summary and conclusions

In this paper we reviewed several algorithms to equalize frequency selective MIMO systems in the space–time-domain. After deriving impulse shortening filters, different constraints have been investigated to allow a memoryless detection due to linear equalizing or decision feedback equalizing. These different schemes were compared by means of Monte-Carlo simulations. Furthermore, the extension of V-BLAST for frequency-selective channels has been regarded. Due to the successive structure and the application of the maximum likelihood sequence equalizer, FS-BLAST outperforms the MIMO-DFE algorithms in the case of short target impulse responses. An additional improvement of the FS-BLAST scheme can be achieved by applying an iterative cancellation scheme denoted as FS-BIC. The performance enhancement of this iterative algorithm compared to FS-BLAST was discussed by simulation results.

Further improvements of the different regarded schemes can be reached by implementing forward error correction codes and soft-input–soft-output equalizers in a turbo-like scheme. In addition, the performance of the several receiver structures should be investigated with respect to non-perfect channel estimation.

References

[1] N. Al-Dhahir, FIR channel-shortening equalizers for MIMO ISI channels, IEEE Trans. Commun. 49 (2) (2001) 213–218.

[2] N. Al-Dhahir, M. Cioffi, Efficiently computed reduced-parameter input-aided MMSE equalizers for ML detection: a unified approach, IEEE Trans. Inf. Theory 42 (3) (1996) 903–915.

[3] N. Al-Dhahir, A. Sayed, A computational efficient MMSE-DFE for multi-user communications, in: Proceedings of the 33rd Annual Asilomar Conference on Signals, Systems, and Computers, Vol. 1, 1999, pp. 207–209.
[4] N. Al-Dhahir, A. Sayed, The finite-length multiple-input multiple-output MMSE-DFE, IEEE Trans. Signal Process. 48 (10) (2000) 2921–2936.
[5] G. Bauch, N. Al-Dhahir, Iterative equalization and decoding with channel shortening filters for space-time coded modulation, in: Proceedings of VTC-Fall, Vol. 3, Boston, USA, 2000, pp. 1575–1582.
[6] G. Bauch, N. Al-Dhahir, Reduced-complexity turbo equalization with multiple transmit/receive antennas over fading multipath channels, in: Proceedings of CISS, Vol. 3, Rhodes, Greece, 2001, pp. 13–18.
[7] A. Benjebbour, H. Murata, S. Yoshida, Performance of iterative successive detection algorithm with space–time transmission, in: Proceedings of IEEE VTC, Vol. 2, Rhodes, Greece, 2001, pp. 1287–1291.
[8] J.M. Cioffi, G.P. Dudevoir, M.V. Eyuboglu, G.D. Forney, MMSE decision-feedback equalizers and coding-Part i: equalization results, IEEE Trans. Commun. 43 (10) (1995) 2582–2594.
[9] C.M. Degen, C.M. Walke, B. Rembold, Comparative study of efficient decision-feedback equalization schemes for MIMO Systems, in: Proceedings of European Wireless'2002, Vol. 2, Florence, Italy, 2002, pp. 793–799.
[10] A. Duel-Hallen, A family of multiuser decision-feedback detectors for asynchronous code-division multiple-access channels, IEEE Trans. Commun. 43 (2/3/4) (1995) 421–434.
[11] D.D. Falconer, F.R. Magee, Adaptive channel memory truncation for maximum likelihood sequence estimation, Bell System Technol. J. 52 (9) (1973) 1541–1562.
[12] G.J. Foschini, Layered space–time architecture for wireless communication in a fading environment when using multiple antennas, Bell Lab. Tech. J. 1 (2) (1996) 41–59.
[13] S. Hayes, Adaptive Filter Theory, 3rd Edition, Prentice-Hall, New York, 1996.
[14] K.D. Kammeyer, Time truncation of channel impulse responses by linear filtering: a method to reduce the complexity of viterbi equalization, Int. J. Electron. Commun. (AEÜ) 48 (5) (1994) 237–243.
[15] K.F. Lee, D.B. Williams, A space-frequency diversity technique for OFDM systems, in: IEEE Proceedings of Globecom'2000, Vol. 3, San Francisco, CA, USA, 2000, pp. 1473-1477.
[16] A. Lozano, C. Papadias, Space-time receivers for wideband BLAST in rich-scattering wire-less channels, in: Proceedings IEEE VTC, Tokyo, Japan, 2000, pp.186–190.
[17] A. Lozano, C. Papadias, Layered space–time receivers for frequency-selective wireless channels, IEEE Trans. Commun. 50 (1) (2002) 65–73.
[18] G.G. Raleigh, J.M. Cioffi, Spatio-temporal coding for wireless communication, IEEE Trans. Commun. 46 (3) (1998) 357–366.
[19] H. Schmidt, K.D. Kammyer, Impulse truncation for wireless OFDM systems, in: Proceedings of 5th International OFDM Workshop, Hamburg, Germany, 2000, pp. 34.1–34.5.
[20] E. Telatar, Capacity of multi-antenna gaussian channels, European Trans. Commun. 10 (6) (1999) 585–595.
[21] W. van Etten, Maximum likelihood receiver for multiple channel transmission systems, IEEE Trans. Commun. 24 (2) (1976) 276–283.
[22] P.W. Wolniansky, G.J. Foschini, G.D. Golden, R.A. Valenzuela, V-BLAST: an architecture for realizing very high data rates over the rich-scattering wireless channel, in: Proceedings of ISSSE'98, Pisa, Italy, 1998, pp. 295–300.
[23] D. Wübben, R. Böhnke, J. Rinas, V. Kühn, K. Kammeyer, Efficient algorithm for decoding layered space–time codes, IEE Electron. Lett. 37 (22) (2001) 1348–1350.
[24] D. Wübben, J. Rinas, R. Böhnke, V. Kühn, K. Kammeyer, Efficient algorithm for detecting layered space–time codes, in: Proceedings of ITG Conference on Source and Channel Coding, Berlin, Germany, 2002, pp. 399–405.